J. Agr. Sci. Tech. (2017) Vol. 19: 231-244

Assessment of Changes in Soil Erosion Risk Using RUSLE in Navrood Watershed, Iran

H. Asadi[1*], M. Honarmand[2], M. Vazifedoust[2], and A. Mousavi[2]

ABSTRACT

Risk assessment of soil erosion, one of the most important land degradation problems worldwide, is very essential for land and water resources management, and development of soil conservation methods. In the present study, the temporal changes of soil erosion risk were assessed from 1987 to 2010, based on the Revised Universal Soil Loss Equation (RUSLE) using Remote Sensing (RS) and Geographic Information Systems (GIS) for the Navrood Watershed, Iran, with an area of 270 km^2. Two Landsat satellite imageries obtained in 1987 and 2010 were used to assess the changes in vegetation cover during this period, and to obtain the Cover factor (C) of RUSLE. Rainfall and soil texture data and a digital elevation model were used to calculate the rest of RUSLE factors, which were taken as constant for the study period. The results showed that the average annual soil loss over the watershed ranged from 0 to 1,056 t ha^{-1} y^{-1} (Cumulative percentage> 99.9%). The area mapped as very high erosion risk (> 100 t ha^{-1} y^{-1}) increased from 10% in 1987 to 12% in 2010, and the area of the next risk class (51-100 t ha^{-1} y^{-1}) increased from 8 to 9%. These changes cover an area of about 800 ha in the watershed, in which erosion risk has been doubled or tripled in the last 23 years. Forest clearing and rangeland overgrazing were identified as the most important reasons for the increase in erosion risk.

Keywords: Forest clearing, Overgrazing, Soil loss, Water erosion, Vegetation cover.

INTRODUCTION

Soil erosion is considered as one of the most important forms of soil degradation worldwide (Oldeman, 1994). The negative effects caused by soil erosion on soil degradation, hydrological systems, agriculture, water quality, and the environment in general have long been established and the impacts of soil erosion continue to pose severe threats to human sustenance (Lal, 1998). Accordingly, assessment of soil erosion hazard is an essential work towards developing erosion prevention methods for lands and water resources management. Erosion risk indicates the relative probability that erosion will occur at a certain location as compared to other locations in the region mapped. Erosion risk maps are constructed using either numerical erosion models or qualitative approaches (Vrieling *et al.*, 2002). Empirical models such as the Universal Soil Loss Equation (USLE) and the Revised Universal Soil Loss Equation (RUSLE) are the most commonly methods (Bhattarai and Dutta, 2007; Zhang *et al.*, 2009) used to predict soil erosion, especially in watershed areas due to their minimal data requirements and ease of application.

USLE/RUSLE predicts the long-term average annual rate of erosion on a field slope, based on rainfall pattern, soil type, topography, crop system, and management

[1] Department of Soil Science, Faculty of Agricultural Engineering and Technology, University of Tehran, Karaj, Islamic Republic of Iran.

[*] Corresponding authore; email: ho.asadi@ut.ac.ir

[2] Department of Soil Science, Faculty of Agricultural Sciences, University of Guilan, Rasht, Islamic Republic of Iran.

practices (soil erosion factors) (Renard *et al.*, 1997). Traditionally, these models were used for local conservation planning at an individual property level. The factors used in these models were usually estimated or calculated from field measurements. The methods of quantifying soil loss based on erosion plots possess many limitations in terms of cost, representativeness, and reliability of the resulting data. They cannot provide spatial distribution of soil erosion loss due to the constraint of limited samples in complex environments. So, mapping soil erosion in large areas is often very difficult using these traditional methods. The use of Remote Sensing (RS) and Geographical Information System (GIS) techniques makes soil erosion estimation and its spatial distribution feasible with reasonable costs and better accuracy in larger areas (Millward and Mersey, 1999; Shi *et al*., 2004; Fu *et al*., 2005; Aydın and Tecimen, 2010; Chen *et al.*, 2011).

The WATEM/SEDEM model (Van Rompaey *et al*., 2001) was recently developed to overcome the shortage of USLE/RUSLE model of predicting sediment delivery. This model calculates 2D-erosion rates using the RUSLE and predicts sediment delivery to river channels using a spatially distributed sediment transport capacity equation. Application of the latest model has been relatively successful in many countries (Van Rompaey *et al*., 2002; 2003, 2005; Verstraeten *et al*., 2007; Alatorre, *et al*., 2010; Shi *et al*., 2012; Haregeweyn *et al*., 2013; Sheng *et al*., 2015; Bezak *et al*., 2015).

Vegetation cover is strongly affected by human activities (Morgan, 2005). Spatial and temporal dynamics of vegetation cover can be assessed by using satellite data, among other methods. A quite common approach is the use of spectral vegetation indices. Vegetation indices, such as *NDVI* (Normalized Difference Vegetation Index) can easily be derived from data acquired by a variety of satellites operating at different spatial resolutions and long time series (Vrieling *et al.*, 2008). The *NDVI* can give a proper relative indication of the spatial and temporal variability of vegetation cover. *NDVI* has therefore often been used for assessing the protective vegetation cover within erosion studies (e.g. De Jong *et al.*, 1999; Jain and Goel, 2002; Symeonakis and Drake, 2004).

Vegetation cover including forests and rangelands has been negatively affected by human activities such as clearing and overgrazing during the last decades across Iran. The objectives of this study were to assess the temporal changes of soil erosion risk during the last two decades in the critical region of Guilan, north part of Iran, based on the Rvised Universal Soil Loss Equation (RUSLE) and using Remote Sensing (RS) and Geographic Information Systems (GIS) in Navrood Watershed.

MATERIALS AND METHODS

Study Area

The study area was Navrood Watershed, located at latitudes between 37. 36 and 37.45 N and longitudes between 48.35 and 48.54 E, in the western part of Guilan Province, in the north of Iran (Figure 1). The area of the watershed is 270 km^2; it drains eastwards to the Caspian Sea. The climate is humid in plain areas and cold in highlands with an annual average precipitation of 836 mm and a mean annual temperature of 10.7^oC. The vegetation cover in this area comprises two types, namely, forest and pasture. The elevation varys from 130 m to 3,000 m. Three soil types, i.e. Alfisols, Entisols and Inceptisols, have been identified in the watershed. Several villages exist in the area.

The RUSLE

The average soil loss due to water erosion per unit area per year was calculated using the RUSLE equation proposed by Renard *et al.* (1997):

$$A = R \times K \times L \times S \times C \times P \quad (1)$$

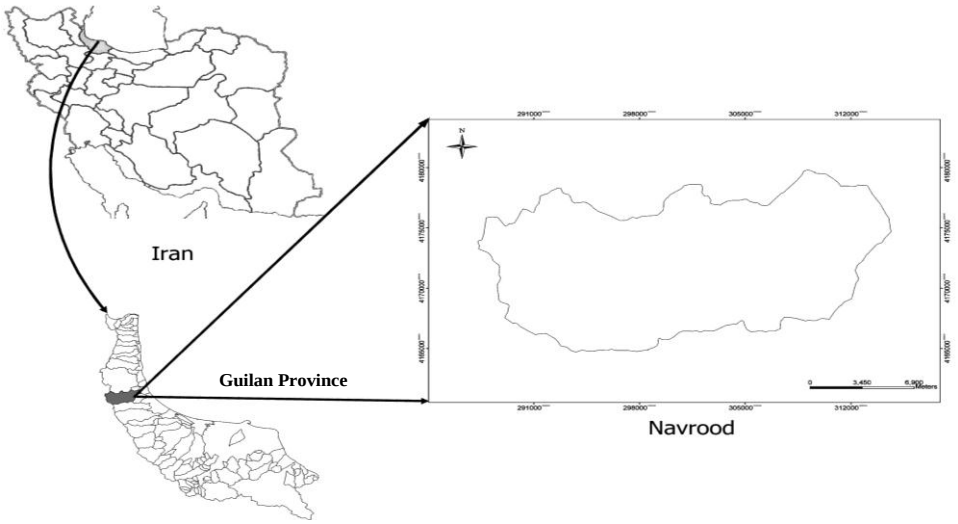

Figure 1. Location of the study area.

Where, *A* is soil loss in t ha^{-1} y^{-1}, *R* is the Rainfall–runoff erosivity factor (MJ mm ha^{-1} h^{-1} y^{-1}), *K* is the soil erodibility factor (t ha h MJ^{-1} ha^{-1} mm^{-1}), *L* is the slope Length factor, *S* is the slope Steepness factor, *C* is the Cover-management practice factor, and *P* is the support Practice factor.

Every erosion factor was converted into a grid layer with a cell size of 90×90 meters. Implementation of the RUSLE in a GIS resulted in annual erosion risk map for the Navrood Watershed.

The RUSLE model uses the Brown and Foster (1987) approach to calculating the average annual rainfall erosivity, *R* (MJ mm ha^{-1} h^{-1} y^{-1}):

$$R = 1/n \sum_{j=1}^{n} \sum_{k=1}^{m_j} (EI_{30})_k \qquad (2)$$

Where, *n* is the number of years of the record, m_j is the number of erosive events for a given year *j*, and EI_{30} is the rainfall erosivity index of a single event k. Thus, *R* factor is the average value of the annual cumulative EI_{30} over a given period. An event's rainfall erosivity EI_{30} (MJ mm ha^{-1} h^{-1}) is calculated as follows:

$$EI_{30} = (\sum e_r v_r).I_{30} \qquad (3)$$

Where, e_r and v_r are, the unit rainfall energy (MJ ha^{-1} mm^{-1}) and the rainfall amount (mm) during a time period *r*, respectively, and I_{30} is the maximum rainfall intensity over a 30 minute period during the event (mm h^{-1}). The unit rainfall energy (e_r) is calculated for each time interval as:

$$e_r = 0.29[1 - 0.72\exp(-0.05i_r)] \qquad (4)$$

Where, i_r is the rainfall intensity during the time interval (mm h^{-1}).

In the current study, rainfall pluviographic data were obtained from nine recording rain gauges in Guilan Province at 15-minutes intervals during the period 2003 to 2007, to generate an erosivity map for the study area. Rainfall erosivity factor (R), average annual precipitation, Fournier index and modified Fournier index (Arnouldus, 1980; Fournier, 1960) were calculated for the nine recording rain gauges, and the correlation between *R* value and these indexes was tested. Then, the equation with the highest correlation was used to estimate *R* value in the other 38 daily-read raingauge stations in Guilan Province. Finally, rainfall erosivity map of the province was produced by kriging method of geostatistic in ArcGIS9.3 (Honarmand *et al*., 2011). The map of R factor for the study area was obtained from the latter map.

To consider early spring erosion by runoff from snowmelt, rainfall erosivity value might be adjusted by adding the precipitation falling through December to March in inches multiplied by 1.5 which gives *R* value in terms of empirical units. This was then multiplyed by 17.02 in order

to obtain the *R* value in MJ mm ha^{-1} h^{-1} y^{-1} (Renard *et al.*, 1997; Whishmeier and Smith, 1978). In this study, firstly, the map of average precipitation from December to March of the province was obtained by kriging method from point data of all 48 stations. The map of snowmelt erosivity was then produced by overlaying this map by the map of snow covered area of the province obtained from MODIS satellite images (Emre Tekeli *et al.*, 2005) and considering the calculation coefficients of 1.5 and 17.02.

Soil erodibility factor was estimated by the relation proposed by Romkens *et al.* (1986):

$$K = 7.594\left\{0.0034 + 0.0405\exp\left[-\frac{1}{2}\left(\frac{\log D_g + 1.659}{0.7101}\right)^2\right]\right\} \quad (5)$$

Where, *K* is in terms of t ha h MJ^{-1} ha^{-1} mm^{-1}, and D_g= Geometric mean particle diameter of soil texture. Values of soil erodibility factor were calculated for each of soil mapping units. As there was no soil map for the watershed, soil unit map was produced by overlaying the geology, topography, land cover and rainfall maps, which yielded 78 units. Finally, 50 surface (0-15 cm) soil samples were collected over the watershed according to the defined soil units, the size of units, and accessibility. Particle size distribution of the soil samples was determined according to Hydrometer Method (Gee and Or, 2002).

In modeling erosion in GIS, it is common to calculate the *LS* combination using the theoretical and technical procedures described by Moore and Burch (1986) and Moore and Wilson (1992). The equation used to compute the *LS* factor is as follows:

$$LS = \left(\frac{A_s}{22.13}\right)^{0.4}\left(\frac{\sin\beta}{0.0896}\right)^{1.3} \quad (6)$$

Where, A_s is the upslope contributing factor per unit width of contour (or rill) in m^2 m^{-1}, β is the slope angle in degrees. In the current work, the Digital Elevation Model (DEM) of the study area with a cell size of 90 m was used to estimate *LS* factor. Slope angle and Flow Direction was determined from DEM. The Flow Direction was used as an input grid to derive the Flow Accumulation that was used to obtain upslope contributing factor.

The Cover and management factor (C) reflects the effect of cropping and management practices on soil erosion rates (Renard *et al.*, 1997). The following formula was used to generate a C factor surface from *NDVI* (Normalized Difference Vegetation Index) values (Van der Knijff *et al.*, 1999, 2000):

$$C = \exp\left(-\alpha\frac{NDVI}{\beta - NDVI}\right) \quad (7)$$

Where, α and β are unitless parameters that determine the shape of the *NDVI-C* curve. An α-value of 2 and a β-value of 1 seem to give reasonable results (Van der Knijff *et al.*, 1999).

In this study, to investigate the temporal changes of soil erosion risk, changes in vegetation cover in two different period were assessed. For this reason, the *C*-factor was calculated using *NDVI* map derived from satellite images. Two Landsat TM images acquired on 10 August 1987 and 2010 with a spatial resolution of 30 m were used to create *NDVI* images.

The *NDVI* was calculated as follows:

$$NDVI = \frac{(NIR - VIS)}{(NIR + VIS)} \quad (8)$$

Where, *VIS* and *NIR* stand for the spectral reflectance measurements acquired in the visible (red) and near-infrared regions, respectively.

In RUSLE, the support Practice (P) factor is generally applied to disturbed lands and represents how surface and management practices, such as contouring, terracing, and strip cropping are used to reduce soil erosion. For areas where there is no support practice, the P factor is set to 1, which was also the case for the study area.

RESULTS AND DISCUSSION

Rainfall+snowmelt erosivity map of the watershed is presented in Figure 2. The rainfall+snow erosivity index ranged from 164 to 1,070 MJ mm ha^{-1} h^{-1} $year^{-1}$ over the

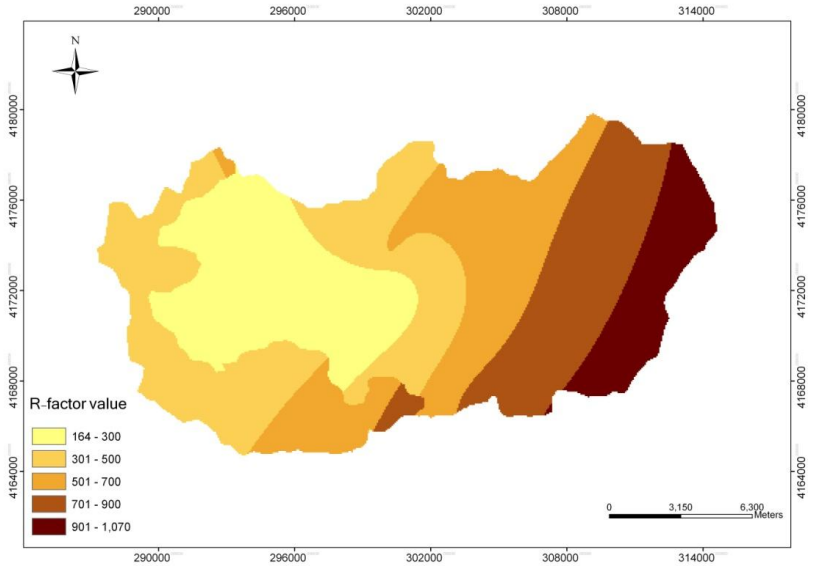

Figure 2. Spatial distribution map of *R*-factor over the watershed.

watershed. Rainfall erosivity relates to rainfall amount and intensity and may be as low as 10 in dry regions (Sepaskhah and Sarkhosh, 2004) to as high as 8,500 in humid regions (Angima *et al*., 2003). Analysis of the spatial variations in *R* factor across Iran (Sadeghi *et al*., 2011) verified that Anzali and Bam Stations, located in the northern and central Iran, respectively, had the maximum and minimum erosivity values, respectively. Angulo-Martínez and Beguería (2009) estimated *R* factor for Ebro Basin of about 85,000 km^2 in the northeastern Spain, to range from 40 to 4,500 MJ mm ha^{-1} h^{-1} $year^{-1}$. In the study of Abu Hammad (2011), *R* ranged from 200 to 450 MJ mm ha^{-1} h^{-1} $year^{-1}$ in a small Mediterranean Watershed in the Central Palestinian Highlands.

The R value followed a decreasing trend from east to west with a slight increase in the western and southwestern regions (Figure 2). Overall, the spatial distribution of the *R* factor in the study area could be explained by the proximity to the major water mass of the Caspian Sea. The relief, with mountain ranges to the west, north, and south of the region, modifies this general pattern. Another effect of the relief is the isolation of the central area from the main precipitation sources through creation of a rain shadow zone. Accordingly, the elevation gradient of rainfall in north of Iran including Guilan Province has been reported to show a second order pattern, which means rainfall decreases to 1,500 m and then increases to 3,000 m (Khalili, 2005). Snow erosivity taking place in mountain areas of southwest and west of the watershed, should also consider in the spatial distribution of the R factor. All these influences result in a rather complex spatial pattern of erosivity.

Soil erodibility varied from 0 to 0.044 t ha h MJ^{-1} ha^{-1} mm^{-1} (Figure 3). Most parts of the study area had *K* values of 0.043-0.044 t ha h MJ^{-1} ha^{-1} mm^{-1} comprising clay and clay loam soils, which classified as high erodibility according to Hazelton (1992). The low *K* values (0-0.0029 t ha h MJ^{-1} ha^{-1} mm^{-1}), which comprised sandy loam soils, were identified in a small area of the watershed (northwest), mostly the region of gravel-sized rock outcrops.

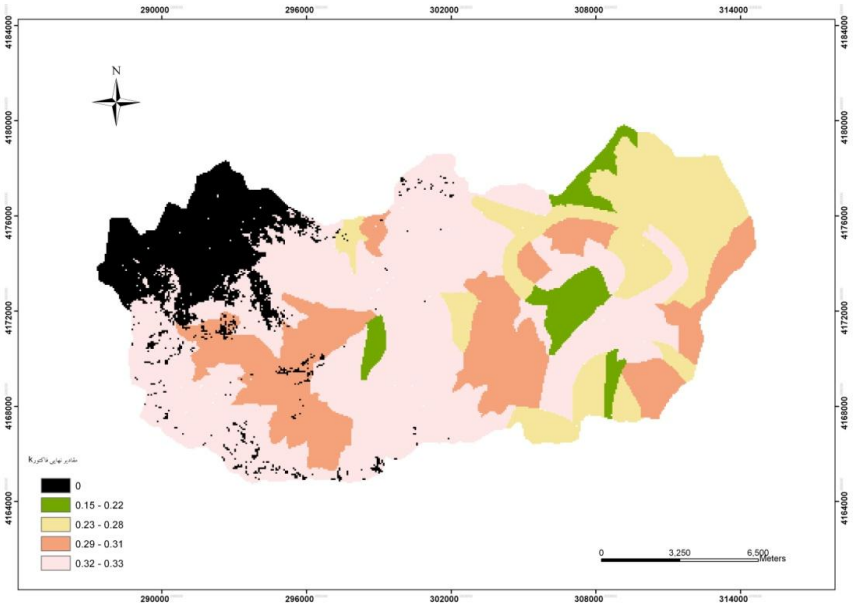

Figure 3. Spatial distribution map of *K*-factor over the watershed.

The *LS*-factor accounts for the effect of slope length and slope gradient on erosion. Soil loss increases more rapidly with slope steepness than it does with slope length (McCool *et al*., 1987). As shown in Figure 4, the topographic factors (LS) ranged from 0 to 259, the steeper the slopes the higher the *LS* factors. The range of *LS* factor and intersection of the classes represents severe topography over the watershed. The watershed has a steep relief (130-3000 m) with mountain ranges to the west, north, and south of the region. The slopes in this watershed also exhibited a complex hillslope profile. The Navrood Watershed represented slopes greater than 10%, many exceeded 50%, and some approached 100% or even more. All these resulted in a higher LS-factor, but, fortunately, most part of the watershed is covered by natural forest shown by low values of *C* factor (Table 1) which prevents very high rates of soil erosion.

In order to prepare C-factor maps, *NDVI* maps were obtained from the Landsat-TM satellite images of the study area. The *NDVI* map showed a range from 0 to 0.73 in 1987 and 0 to 0.74 in 2010. The C values derived from the *NDVI* map ranged from 0.003 to 1 in both years. Generally, eastern regions of the watershed with lowest *C* values are covered by dense forest; on the other hand, northwestern region of the watershed with bare soils and rocks shows highest *C* values. To give an insight into the situation, five classes were defined for the C value and the area coverage was derived for each class in both years of 1987 and 2010 (Table 1). The first class (C< 0.15) including undisturbed forests and pasture/rangelands with more than 40% ground cover has been decreased from 72 to 68% of the total watershed area, i.e. 1,080 ha of the forest/rangelands has been cleared/overgrazed during this period. On the other hand, the area of the *C* class of 0.85-1, which represents bare soils and rock outcrops, has been increased from 5 to 6.8 percent of the watershed, i.e. about 486 ha

Table 1. Area coverage (%) of each class of *C* values in two differrent periods.

C Value	0.003-0.15	0.15-0.3	0.3-0.5	0.5-0.85	0.85-1
1987	72.03	5.64	4.95	12.32	5.06
2010	68.09	8.17	6.96	9.96	6.82

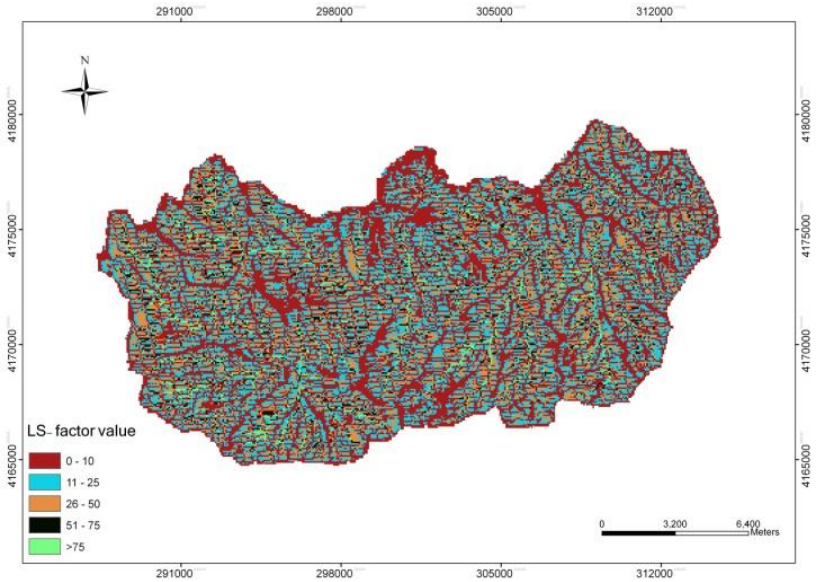

Figure 4. Spatial distribution map of *LS*-factor values over the watershed.

has been added to the area of bare soils. All these changes resulted in higher erosion risk, as discussed below.

Prediction of the average annual soil loss (soil erosion risk) was computed by overlaying five maps of RUSLE factors in ArcGIS for the two dates (Figures 5 and 6). Results show that the average annual soil loss over the watershed ranged from 0 to more than 100 t ha^{-1} y^{-1} in both priods. The lowest erosion risk corresponds to the area of rock outcrops of northwestern part of the watershed, and to undisturbed dense forests extended from east to central region of the watershed. In contrast, the highest soil erosion risk of > 100 t ha^{-1} y^{-1} corresponded to bare soils of rangelands of the watershed mostly located in western parts of steep slopes.

Annual soil loss (erosion risk) was classified into four different classes of low, moderate, high, and very high erosion risk of

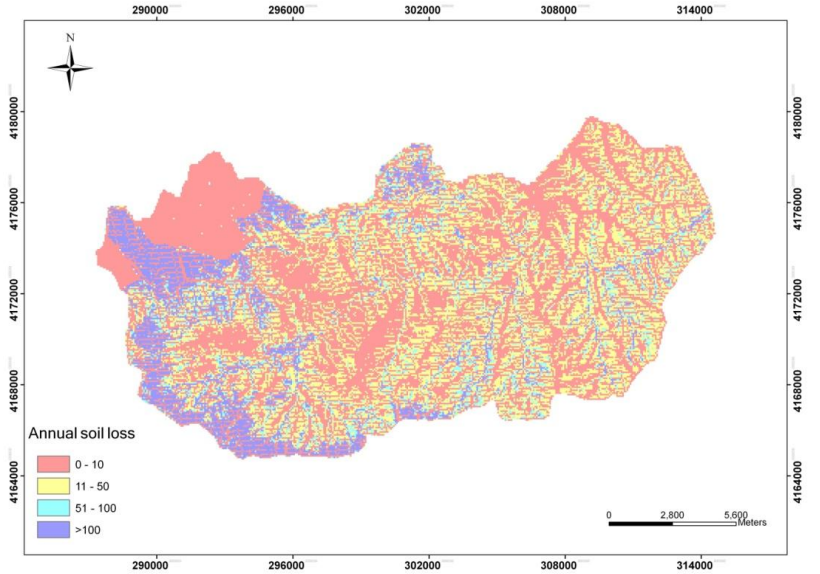

Figure 5. Spatial distribution map of average annual soil loss over the watershed in 1987.

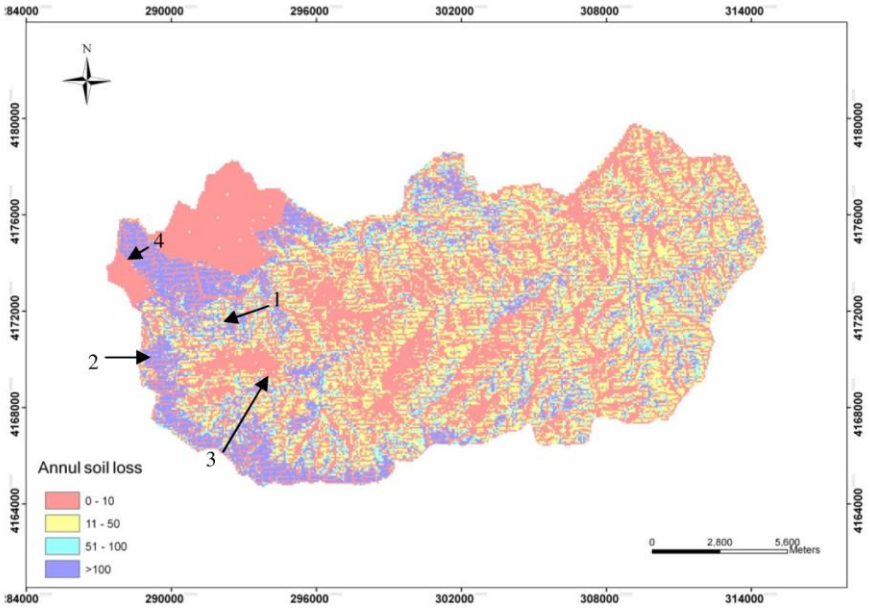

Figure 6. Spatial distribution map of average annual soil loss over the watershed in 2010.

0-10, 11-50, 51-100 and > 100 t ha^{-1} y^{-1}, respectively. This allows simple calculations/comparisions of the area coverage and ratios of the classes for two years of prediction. The area coverage and relative percent of each class were derived from the soil erosion map of the study area in both years of 1987 and 2010. Grouping of erosion risks in different classes has also been carried out by Prasuhn *et al*. (2013) following the German Direct Support Scheme Obligation Regulations in which three classes of low (0-30), moderate (30-55) and high (> 55) are defined.

The lowest erosion risk (0–10 t ha^{-1} y^{-1}) comprised 53% of the total area in 1987 and remained almost the same in 2010. The area of moderate erosion risk (11-50 t ha^{-1} y^{-1}), which extended mainly over the valley sides and disturbed sites in the watershed, decreased from 29% in 1987 to 26% in 2010. On the other hand, the area of high (51-100 t ha^{-1} y^{-1}) and very high (> 100 t ha^{-1} y^{-1}) erosion risks increased from 8 to 9% and from 10 to 12%, respectively. This means that the erosion risk of about 800 ha of the watershed area increased two to more than three times during 23 years. Forest clearing and rangeland overgrazing are the most important reasons of these changes. In an opposite situation at Kuseyr Plateau, Turkey, Ozsahin and Uygur (2014) showed that the land under severe erosion risk decreased from 30 to 22% from 1987 to 2010. The maximum and average annual soil losses in the plateau were as high as 59.81 and 6.19 t ha^{-1} per year in 1987, respectively, and 48.33 and 5.00 t ha^{-1} per year in 2010, respectively. Reclamation of the land cover from the past to the present was mentioned as the key factor in this regard. In other studies, the change of land use and land cover was used to calculate either historical (Mutekanga *et al*., 2010) or future erosion risk (Prasuhn *et al*., 2013). Also, the possible reduction of soil erosion risk was estimated by Karydas *et al*. (2009) and the erosion risk of environmental changes was evaluated by Zhang *et al*. (2010).

Validation of spatial soil loss predictions through soil erosion models and, therefore, validation of soil erosion risk maps are generally difficult (Gobin *et al*., 2004; Prasuhn *et al*., 2013). There is a lack of scale-specific calibration and validation data (Tetzlaff *et al*., 2013). Spatial predictions should also be verified through spatial, field-based assessments of soil erosion (Bui *et al*.,

2011). However, there is very few such data; the majority of data are outlet based, e.g. measurements of sediment load of rivers. Additionally, long-term measurement series from actually cultivated plots are required to verify the long-term average soil loss (Prasuhn *et al*., 2013). Accordingly, validation of the obtained map was carried out qualitatively just with visual survey. There was a spatially good agreement between mapped soil loss and field observation of soil erosion/cover, particularly for the area with potentially low and very high erosion risks (Figure 7).

The map of potential erosion risk (Figure 8) was produced by setting *C* factor to 1, based on the assumption of vegetation cover clearing. Potential erosion risk is defined as the inherent risk of erosion irrespective of current land use or vegetation cover (Vrieling *et al*., 2002). According to the map, the potential erosion risk ranged from 0 to over 400 t ha^{-1} y^{-1}. The result show that vegetation cover has an important role in preventing soil loss in 57% of the watersed that has high to very high potential soil erosion risk of more than 400 t ha^{-1} y^{-1}. The area with very high potential erosion risk extended mainly over the east part of the watershed where the current actual erosion risk is low (Figure 6) . It is a fact that rainfall erosivity is high over the Navrood Watershed and its topography is very steep, therefore, vegetation cover plays an important role in controlling soil erosion. It will result in very high erosion if the vegetation cover, especially forests, is removed by clearing or fire.

The average soil erosion rates estimated for the watershed accorded with similar studies carried out in different parts of the world. Shi *et al*. (2002) estimated average annual soil loss for Hanjiang River in central China with the area of 45,000 km^2 to be from zero to > 80 t ha^{-1} per year. In an agricultural catchment in central Kenyan highland conditions, for segments with *LS*-factors between 0 and 10, Angima *et al*. (2003) predicted the average soil loss to be 134 t ha^{-1} per year, while for *LS*-factors

Figure 7. Four examples for plausibility checks of the soil loss map in the field. The number and arrows show the location and direction of photography indicated in Figure 6.

between 10 and 20, predicted soil loss increased to 420 t ha^{-1} per year, and for slopes with *LS*-factors between 20 and 30, the predicted soil loss was 549 t ha^{-1} per year. Abu Hammad (2011) estimated that soil loss ranged from 0 to > 50 t ha^{-1} y^{-1} in a small Mediterranean Watershed in the central Palestinian highlands. Prasannakumar *et al*. (2012) estimated the average soil erosion rate for a forested mountainous sub-watershed in Kerala, India, to be from 0 to 17.73 t h^{-1} y^{-1}. Prasuhn *et al*. (2013) used a similar methodology to obtaine the soil erosion risk map of Switzerland. They estimated actual soil loss for agricultural area and permanent grassland to be approximately > 50 and > 10 t ha^{-1} y^{-1}, respectively, while the potential

erosion risk was estimated to be > 500 t ha^{-1} y^{-1}.

Finally, identification of areas with high risk of soil loss (Figures 5 and 6) necessitated the application of certain conservation and management practices. As the area with high risk of soil erosion are mainly the ranges of upland consisting of steep and hilly areas, the easy and affordable conservation practices to control the high soil loss rate are vegetation cover and grazing management. On the other hand, considering the high rainfall erosivity (Figure 2) and the steep topography (Figure 4) of the region, any change in vegetation cover, especially forest clearing, should be strictly prevented, otherwise the rate of soil erosion will increase several times over the whole watershed (Figure 8). Optimizing land use while implementing legal restrictions will lead to a decrease in erosion rate (Vafakhah and Mohseni Saravi, 2011).

CONCLUSIONS

This study attempted to asses soil erosion risk and to map changes in Navrood Watershed, north of Iran, betweein 1987 and 2010 by implementing RUSLE in a GIS environment. This approach proved to be an effective way to map the spatial distribution of soil erosion risks in a large area and could be an efficient, easy, and time-saving method for soil erosion risk monitoring. Moreover, the results indicated those locations in the watershed that were susceptible to high risks of soil erosion. Therefore, in accordance with the current land uses, appropriate conservation measures could be adopted by the pertinent authorities and organizations.

In the Navrood Watershed, the land use pattern in areas prone to soil erosion indicates that areas with natural forest cover in the most eastern parts of the watershed have minimum rate of soil erosion while areas with overgrazed range covers have high rate of soil erosion (> 50 t h^{-1} y^{-1}). Terrain alterations along with high *LS*-factor and rainfall prompt these areas to be more susceptible to soil erosion. The predicted amount of soil loss and its spatial distribution can provide a basis for comprehensive management and sustainable land use for the watershed. The areas with high and severe soil erosion warrant special priority for the implementation of control measures. While the present analytical model helps mapping of vulnerability zones,

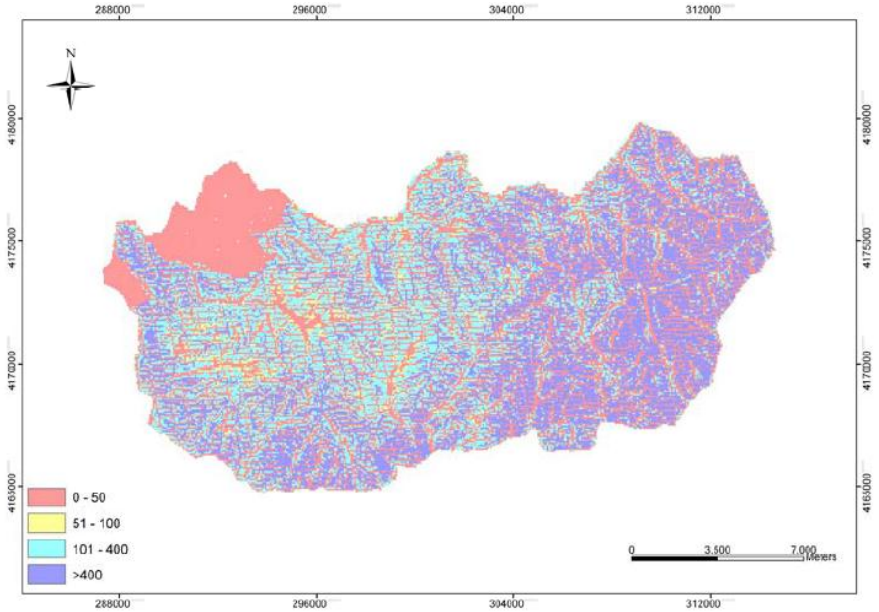

Figure 8. Spatial distribution map of potential erosion risk over the watershed.

micro-scale data on rainfall intensity, soil texture and field measurements can augment the prediction capability and accuracy of remote sensing and GIS based analysis. During the studied 23 years (1987-2010), the erosion risk of about 3% of the watershed area increased from moderate (11-50 t ha^{-1} y^{-1}) to high (51-100 t ha^{-1} y^{-1}) and very high (> 100 t ha^{-1} y^{-1}). This area extended mainly over the watershed valley sides and disturbed sites. Forest clearing and rangeland overgrazing seem to be the most important reasons of these changes.

The map of potential erosion risk, as the inherent risk of erosion irrespective of current land use or vegetation cover, show that vegetation cover has an important role in preventing soil loss in 57% of the watersed that had high to very high potential of soil erosion risk of more than 400 t ha^{-1} y^{-1}. Removal of the vegetation cover by clearing or fire will result in very high soil erosion. It is a fact that rainfall erosivity is high over the Navrood Watershed and its topography is very steep, therefore, vegetation cover plays an important role in preventing soil erosion.

ACKNOWLEDGEMENTS

Authors would like to acknowledge Guilan Water Company for financial support of the project.

REFERENCES

1. Abu Hammad, A. 2011. Watershed Erosion Risk Assessment and Management Utilizing Revised Universal Soil Loss Equation-Geographic Information Systems in the Mediterranean Environments. *Water Environ. J.*, **25(2):** 149-162.
2. Alatorre, L. C., Beguería, S. and García-Ruiz, J. M. 2010. Regional Scale Modeling of Hillslope Sediment Delivery: A Case Study in the Barasona Reservoir Watershed (Spain) Using WATEM/SEDEM. *J. Hydrol.*, **391(1):** 109-123.
3. Angima, S. D., Stott, D. E., O'Neill, M.K., Ong, C. K. and Weesies, G. A. 2003. Soil Erosion Prediction Using RUSLE for Central Kenyan Highland Conditions. *Agric. Ecosyst. Environ.*, **97:** 295-308.
4. Angulo-Martínez, M. and Beguería, S. 2009. Estimating Rainfall Erosivity from Daily Precipitation Records: A Comparison among Methods Using Data from the Ebro Basin (NE Spain). *J. Hydrol.*, **379**: 111-121.
5. Arnouldus, H. M. J. 1980. An Approximation of the Rainfall Factor in the Universal Soil Loss Equation. In: "*Assessment of Erossion*", (Eds.): De Boodt, M. and Gabriels, D.. Chichester, New York, PP. 127-132.
6. Aydın, A. and Tecimen, H. B. 2010. Temporal Soil Erosion Evaluation: A CORINE Methodology Application at Elmalı Dam Watershed, Istanbul. *Environ. Earth Sci.*, **61:** 1457-1465.
7. Bezak, N., Rusjan, S., Petan, S., Sodnik, J. and Mikos, M. 2015. Estimation of Soil Loss by the WATEM/SEDEM Model Using an Automatic Parameter Estimation Procedure. *Environ. Earth Sci.*, **74:** 5245–5261.
8. Bhattarai, R. and Dutta, D. 2007. Estimation of Soil Erosion and Sediment Yield using GIS at Catchment Scale. *Water Resour. Manage.*, **21:** 1635-1647.
9. Brown, L. C. and Foster, G. R. 1987. Storm Erosivity Using Idealized Intensity Distributions. *Trans. ASAE*, **30:** 379-386.
10. Bui, E. N., Hancock, G. J. and Wilkinson, S. N. 2011. Tolerable Hillslope Erosion Rates in Australia. Linking Science and Policy. *Agric., Ecosyst. Environ.*, **144:** 136-149.
11. Chakroun, H., Bonn, F. and Fortin, J. P. 1993. Combination of Single Storm Erosion and Hydrological Models into a Geographic Information System. In: "*Farm Land Erosion: In Temperate Plains Environment and Hills*", (Ed.): Wicherek, S.. Elsevier, Amsterdam, PP. 261-270.
12. Chen T., Niu, R.Q., Li, P. X., Zhang, L. P. and Du, B. 2011. Regional Soil Erosion Risk Mapping Using RUSLE, GIS, and Remote Sensing: A Case Study in Miyun Watershed, North China. *Environ. Earth Sci.*, **63:** 533–541.
13. De Jong, S. M., Paracchini, M. L., Bertolo, F., Folving, S., Megier, J. and De Roo, A. P. J. 1999. Regional Assessment of Soil Erosion Using the Distributed Model SEMMED and Remotely Sensed Data. *Catena*, **37(3/4):** 291–308.

14. Emre-Tekeli, A., Akyurek, Z., Arda Sorman, A., Sensoy, A. and Unal-Sorman, A. 2005. Using MODIS Snow Cover Maps in Modeling Snowmelt Runoff Process in the Eastern Part of Turkey. *Remote Sens. Environ.*, **97:** 216- 230.
15. Fournier, F. 1960. *Climat et Erosion.* Presses Universitaires de France, Paris.
16. Fu, B. J., Zhao, W. W., Chen, L. D., Zhang, Q. J., Lü, Y. H., Gulinck, H. and Poesen, J. 2005. Assessment of Soil Erosion at Large Watershed Scale Using RUSLE and GIS: A Case study in the Loess Plateau of China. *Land Degrad. Dev.*, **16(1):** 73-85.
17. Gee, G. W. and Or, D. 2002. Particle-Size Analysis. Part 4. In: "*Methods of Soil Analysis*", (Eds.): Dane, J. H. and Topp, C. SSSA, Madison, WI, PP. 255-289.
18. Gobin, A., Jones, R., Kirkby, M., Campling, P., Govers, G., Kosmas, C. and Gentile, A. 2004. Indicators for Pan-European Assessment and Monitoring of Soil Erosion by Water. *Environ. Sci. Policy*, **7:** 25-38.
19. Haregeweyn, N., Poesen, J., Verstraeten, G., Govers, G., de Vente, J., Nyssen, J., Deckers, J. and Moeyersons, J. 2013. Assesing the Preformance of Aspatially Distributed Soil Erosion and Sediment Delivery Model (WATEM/SEDEM) in Northern Ethiopia. *Land Degrad. Dev.*, **24:** 188–204.
20. Hazelton, P. A. 1992. Soil Landscapes of the Kiama 1:100,000 sheet. Department of Conservation and Land Management (Incorporating the Soil Conservation Service of NSW), Sydney.
21. Honarmand, M., Asadi, H., Vazifedoost, M. and Moussavi, A. 2011. Rainfal Erosivity Index in Guilan Province. *Proceeding of the 12th Iranian Soil Science Congress*, 12-15 July 2011, Tabriz University, Tabriz, Iran.
22. Jain, S. K. and Goel, M. K. 2002. Assessing the Vulnerability to Soil Erosion of the Ukai Dam Catchments Using Remote Sensing and GIS. *Hydrol. Sci. J.*, **47(1):** 31-40.
23. Karydas, Ch. G., Sekuloska, T. and Silleos, G.N. 2009. Quantification and Site-Pecification of the Support Practice Factor When Mapping Soil Erosion Risk Associated with Olive Plantations in the Mediterranean Island of Crete. *Environ. Monit. Assess.*, **149(1-4):** 19–28.
24. Khalili, A. 2005. The Climate of Iran. In: "*The Soils of Iran, new achievements in perception, management and use*", (Eds.): Banaei, M. H., Moameni, A., Bybordi, M. and Malakouti, M. JIranian Soil and Water Research Institute, Sana Publication, Iran, **1(3):** 24-71.
25. Lal, R. 1998. Soil Erosion Impact on Agronomic Productivity and Environment Quality: Critical Reviews. *Plant Sci.*, 17: 319-464.
26. McCool, D. K., Brown, L. C., Foster, G. R., Mutchler, C. K. and Meyer, L. D. 1987. Revised Slope Steepness Factor for the Universal Soil Loss Equation. *Trans. ASAE*, **30:** 1387-1396.
27. Millward, A. A. and Mersey, J. E. 1999. Adapting the RUSLE to Model Soil Erosion Potential in a Mountainous Tropical Watershed. *Catena*, **38:** 109-129.
28. Moore, I. D. and Burch, G. J. 1986. Physical Basis of the Length-slope Factor in the Universal Soil Loss Equation. *Soil Sci. Soc. Am. J.*, **50:** 1294-1298.
29. Moore, I. D. and Wilson, J. P. 1992. Length-slope Factors for the Revised Universal Soil Loss Equation: Simplified Method of Estimation. *J. Soil Water Conserv.*, 47: 423-428.
30. Morgan, R. P. C. 2005. *Soil Erosion and Conservation*. Third Edition, Blackwell Publishing Ltd, Oxford, UK, 304 PP.
31. Mutekanga, F. P., Visser, S. M. and Stroosnijder, L. 2010. A Tool for Rapid Assessment of Erosion Risk to Support Decision-making and Policy Development at the Ngenge Watershed in Uganda. *Geoderma*, **160(2):** 165–174.
32. Oldeman, L. R. 1994. The Global Extent of Soil Degradation. In: "*Soil Resilience and Sustainable Landuse*", (Eds.): Greenland, D. J. and Saboles, T. Commonwealth Agricultural Bureau International, Wallingford, UK.
33. Ozsahin, E. and Uygur, V. 2014. The Effects of Land Use and Land Cover Changes (LULCC) in Kuseyr Plateau of Turkey on Erosion. *Turk. J. Agric. For.*, **38:** 478-487.
34. Prasuhna, V., Liniger, H., Gisler, S., Herweg, K., Candinas, A. and Clément, J.P. 2013. A High-resolution Soil Erosion Risk Map of Switzerland as Strategic Policy Support System. *Land Use Policy*, 32: 281-291.
35. Renard, K. G., Foster, G. R., Weesies, G. A., McCool, D. K. and Yoder, D. C. 1997. *Predicting Soil Erosion by Water: A Guide to Conservation Planning with the Revised*

Universal Soil Loss Equation (RUSLE). Agriculture Handbook No. 703, USDA, Washington, DC, USA. 404 PP.
36. Prasannakumar, V., Vijith, H., Abinod, S. and Geetha, N. 2012. Estimation of Soil Erosion Risk within a Small Mountainous Sub-watershed in Kerala, India, Using Revised Universal Soil Loss Equation (RUSLE) and Geo-information Technology. *Geosci. Front.*, **3(2):** 209-215.
37. Romkens, M. J. M., Prased, S. N. and Poesen, J. W. A. 1986. Soil Erodibility and Properties. *Proceeding 13th Congress of the Intern. Soc. of Soil*, Homburg, Germany, **5:** 492-504.
38. Sadeghi, S. H. R., Moatamednia, M. and Behzadfar, M., 2011. Spatial and Temporal Variations in the Rainfall Erosivity Factor in Iran. *J. Agr. Sci. Tech.*, 13: 451-464.
39. Sepaskhah, A. R. and Sarkhosh, P. 2004. Estimating Storm Erosion Index in Southern Region of Islamic Republic of Iran. *Iran. J. Sci. Tech., Trans. B Eng.*, **29(B3).**
40. Sheng, M., Fang, H. and Guo, M. 2015. Modeling Soil Erosion and Sediment Yield Using WaTEM/SEDEM Model for the Black Soil Region of Northeast China. *Resou. Sci.*, **37(4):** 815-822.
41. Shi, Z. H., Ai, L., Fang, N. F. and Zhu, H. D. 2012. Modeling the Impacts of Integrated Small Watershed Management on Soil Erosion and Sediment Delivery: A Case Study in the Three Gorges Area, China. *J. Hydrol.*, 438: 156-167.
42. Shi, Z. H., Cai, C. F., Ding, S. W., Li, Z. X., Wang, T. W. and Sun, Z. C. 2002. Assessment of Erosion Risk with the Rusle and Gis in the Middle and Lower Reaches of Hanjiang River. *12th ISCO Conference*, May 26-31, 2002, Beijing, China.
43. Shi, Z. H., Cai, C. F., Ding, S. W., Wang, T. W. and Chow, T. L. 2004. Soil Conservation Planning at the Small Watershed Level Using RUSLE with GIS: a Case Study in the Three Gorge Area of China. *Catena*, **55(1):** 33-48.
44. Symeonakis, E. and Drake, N. 2004. Monitoring Desertification and Land Degradation over Sub-Saharan Africa. *Int. J. Remote Sens.*, **25(3):** 573-592.
45. Tetzlaff, B., Friedrich, K., Vorderbrügge, T., Vereecken, H. and Wendland, F. 2013. Distributed Modelling of Mean Annual Soil Erosion and Sediment Delivery Rates to Surface Waters. *Catena*, **102:** 13-20.
46. Vafakhah, M. and Mohseni Saravi, M., 2011. Optimizing Management of Soil Erosion in Orazan Sub-basin Iran. *J. Agr. Sci. Tech.*, **13:** 717-726.
47. Van der Knijff, M., Jones R. J. A. and Montanarella, L. 1999. *Soil Erosion Risk in Italy: EUR19022 EN*. Office for Official Publications of the European Communities, Luxembourg, 54 PP.
48. Van der Knijff, M., Jones R. J. A. and Montanarella, L. 2000. *Soil Erosion Risk Assessment in Europe: EUR 19044 EN*. Office for Official Publications of the European Communities, Luxembourg, 34 PP.
49. Van Rompaey, A., Bazzoffi, P., Jones, R. J. A. and Montanarella, L. 2005. Modelling Sediment Budgets in Italian Catchments. *Geomorphol.*, **65:** 157–169.
50. Van Rompaey, A., Govers, G. and Puttemans, C. 2002. Modelling Land Use Changes and Their Impact on Soil Erosion and Sediment Supply to Rivers. *Earth Surf. Proc. Land.*, **27**: 481–494.
51. Van Rompaey, A., Krasa, J., Dostal, T. and Govers, G. 2003. Modelling Sediment Supply to Rivers and Reservoirs in Eastern Europe during and after the Collectivization Period. *Hydrobiologia*, **494:** 169–176.
52. Van Rompaey, A., Verstraeten, G., Van Oost, K., Govers, G. and Poesen, J. 2001. Modelling Mean Annual Sediment Yield Using a Distributed Approach. *Earth Surf. Proc. Land.*, **26:** 1221–1236.
53. Verstraeten, G., Prosser, I. P. and Fogarty, P. 2007. Predicting the Spatial Patterns of Hillslope Sediment Delivery to River Channels in the Murrumbidgee Catchment. *Australia J. Hydrol.*, **334:** 440–454.
54. Vrieling, A., de Jong, S. M., Sterk, G. and Rodrigues, S. C. 2008. Timing of Erosion and Satellite Data: A Multi-resolution Approach to Soil Erosion Risk Mapping. *Int. J. Appl. Earth Observ. Geoinfo.*, **10**: 267-281.
55. Vrieling, A., Sterk, G. and Beaulieu, N. 2002. Erosion Risk Mapping: A Methodological Case Study in the Colombian Eastern Plains. *J. Soil Water Conserv.*, **57(3):** 158-163.
56. Whishmeier, W. H. and Smith, D. D. 1978. *Predicting Rainfall Erosion Losses: A Guide to Soil Conservation Planning*. Handbook No. 537. US Department of Agriculture U.S.

Department of Agriculture, Washington, D.C.
57. Zhang, X., Wu, B., Ling, F., Zeng, Y., Yan, N. and Yuan, Ch. 2010. Identification of Priority Areas for Controlling Soil Erosion. *Catena*, **83(1):** 76–86.
58. Zhang, Y., Degroote, J., Wolter, C. and Sugumaran, R. 2009. Integration of Modified Universal Soil Loss Equation (MUSLE) into a GIS Framework to Assess Soil Erosion Risk. *Land Degrad. Dev.*, **20:** 84-91.

ارزیابی تغییرات خطر فرسایش خاک با استفاده از RUSLE در حوضه ناورود، ایران

ح. اسدی، م. هنرمند، م. وظیفه‌دوست و ع. موسوی

چکیده

ارزیابی خطر فرسایش خاک، به عنوان کی از مهم‌ترین مشکلات تخریب خاک در سراسر جهان، برای مدیریت منابع آب و خاک و توسعه روش‌های حفاظت خاک ضروری است. در مطالعه حاضر، تغییرات زمانی خطر فرسایش خاک از سال ۱۳۶۶ تا ۱۳۸۹ بر اساس معادله جهانی هدررفت خاک تجدیدنظر شده (RUSLE) با بهره‌گیری از سامانه اطلاعات جغرافیایی (GIS) و سنجش از دور (RS) در حوضه ناورود ایران با مساحت ۲۷۰ کیلومتر مربع ارزیابی شد. دو تصویر ماهواره‌ای مربوط به سال‌های ۱۳۶۶ و ۱۳۸۹ برای ارزیابی تغییرات پوشش گیاهی در این مدت، و تعیین فاکتور پوشش گیاهی (C) مدل RUSLE مورد استفاده قرار گرفت. داده‌های بارندگی، بافت خاک و مدل رقومی ارتفاع برای محاسبه سایر فاکتورهای مدل به کار رفته و برای دوره مورد نظر ثابت فرض شدند. نتایج نشان داد که میانگین سالانه تلفات خاک در سطح حوضه از صفر تا ۱۰۵۶ تن در هکتار در سال (با فراوانی تجمعی بیش از ۹۹/۹ درصد) متغییر است. سطح مناطق با خطر فرسایش خیلی زیاد (بیش از ۱۰۰ تن در هکتار در سال) از ۱۰ درصد در سال ۱۳۶۶ به ۱۲ درصد در سال ۱۳۸۹ افزایش یافته است. سطح مناطق در کلاس بعدی خطر فرسایش (۵۱ تا ۱۰۰ تن در هکتار در سال) نیز از ۸ به ۹ درصد افزایش داشته است. این تغییرات مرتبط با سطحی در حدود ۸۰۰ هکتار است که در آن و در طی ۲۳ سال، خطر فرسایش خاک دو تا سه برابر شده است. جنگل‌تراشی و چرای بی‌رویه مراتع از مهم‌ترین دلایل این افزایش، تشخیص داده شدند.